Stress analysis of a suspension control arm

Paula Andrea Chacón Santamaría, Alejandro Sierra, Octavio Andrés González Estrada

ESCUELA DE INGENIERÍA
MECÁNICA

Universidad Industrial de Santander

RESEARCH REPORT

STRESS ANALYSIS OF A SUSPENSION CONTROL ARM

Paula Andrea Chacón Santamaría
Alejandro Sierra
Octavio Andrés González-Estrada

A010
Bucaramanga 2018

Research Group on Energy and Environment – GIEMA
School of Mechanical Engineering
Universidad Industrial de Santander

P A Chacón Santamaría, A Sierra, O A González-Estrada, *Stress analysis of a suspension control arm*, School of Mechanical Engineering, Universidad Industrial de Santander. Research report, Bucaramanga, Colombia, 2018.

Abstract: The suspension system of a vehicle absorbs energy to cushion and soften displacements in irregular terrains, and also supports its bodywork. Some of the components that allow the correct performance of the system are the control arms. This work aims to determine the stress distribution of a control arm for the rear suspension of a buggy vehicle. The suspension geometry was modelled in order to find the loads applied on the control arm through a movement analysis. As a result, the loads were obtained as a function of time, from these values two critical times were selected to perform the analyses. The maximum von Mises stresses were evaluated as 22 MPa and 20 MPa for each time, which are low values considering the strength of the material used to manufacture these parts.

Keywords: boundary conditions; control arm; finite element method; von Mises stress.

Correspondence: agonzale@uis.edu.co

Research Group on Energy and Environment – GIEMA
School of Mechanical Engineering
Universidad Industrial de Santander
Ciudad Universitaria
Bucaramanga, Colombia

email: giema@uis.edu.co http://giema.uis.edu.co

Stress analysis of a suspension control arm

P. Chacón[1], A Sierra[2], O A González-Estrada[1]

[1] GIEMA, Universidad Industrial de Santander, Bucaramanga, Colombia. Email: p_chacon96@hotmail.com, agonzale@uis.edu.co
[2] Servicio Nacional de Aprendizaje - SENA, Bucaramanga, Colombia

ABSTRACT

The suspension system of a vehicle absorbs energy to cushion and soften displacements in irregular terrains, and also supports its bodywork. Some of the components that allow the correct performance of the system are the control arms. This work aims to determine the stress distribution of a control arm for the rear suspension of a buggy vehicle. The suspension geometry was modelled in order to find the loads applied on the control arm through a movement analysis. As a result, the loads were obtained as a function of time, from these values two critical times were selected to perform the analyses. The maximum von Mises stresses were evaluated as 22 MPa and 20 MPa for each time, which are low values considering the strength of the material used to manufacture these parts.

KEYWORDS: boundary conditions; control arm; finite element method; von Mises stress.

1. INTRODUCTION

In the research group GIEMA, we have considered fundamental challenges of engineering to define the research lines of the group, as proposed by UNESCO. We focus on sustainable development goals, and include, e.g., research on new materials [1]–[4], affordable and clean energy [5]–[8], industry innovation [9]–[11], good health and wellbeing [12]. Regarding industry innovation, it is important to take advantage of novel approaches to manufacture and design, which allow the use of computational tools [13] to improve the design cycle of mechanical components, especially in sensitive sectors as the automotive industry.

The suspension system of a car is the set of elements that links the sprung elements of a vehicle with the unsprung ones. There are different models depending on the mechanisms used. Suspension systems are generally divided into two groups: dependent and independent [14]. The selected vehicle has a double A-arm system, which is independent. This means that each wheel is isolated from the others movement. A spring shock absorber controls the movement of the assembly. This suspension type is characterised by having two control arms, the upper one and the lower one. Usually, both arms are the same length but there is an arrangement frequently known as Short Long Arm suspension, for which the upper arm is usually shorter. The control arms are the elements that connect the chassis with the ball joints. These arms support the spring shock absorber and are part of the four-bar linkage that establishes the correct movement of the system. Each suspension component ensures the contact of the wheels with the ground, allowing relative movement between the wheels and the chassis [15].

Therefore, a suspension system in poor conditions, with excessive wear or wrong designed, cannot maintain the stability of the vehicle. In this sense, Finite Element Analysis (FEA) allows to design mechanical parts by estimating their mechanical response to loading conditions [16]. In this work, the stress distribution of the lower control arm of a small vehicle is calculated using the software Ansys. First, the methodology that was followed is described, detailing the formulation of the problem, the procedures used for calculation and the post-processing. Then, the results of the calculated loads, von Mises stress and total deformation distributions are shown. Finally, conclusions are presented.

2. METHODOLOGY

To perform a stress analysis, the usual procedure for solving problems using FEM was followed, which is divided into three steps: pre-processing, calculation and post-processing.

2.1. Material and geometry

The response of the suspension system of a buggy car was studied since these vehicles are frequently used in roads with irregularities. The material of the lower control arm, the component considered for the study, is steel, with properties shown in Table 1. This material is one of the most used to manufacture this mechanical part in commercial automobiles, followed by aluminium alloys.

Table 1. Structural steel mechanical properties.

Property	**Value**
Tensile ultimate strength	460 MPa
Tensile yield strength	250 MPa
Young's modulus	2×10^{11} Pa
Poisson's ratio	0.3
Bulk modulus	1.6667×10^{11} Pa
Shear modulus	7.6923×10^{10} Pa

Source. Ansys database.

The geometry of the part is shown in Figure 1. For the accurate calculation of the stress distribution, this geometry should be as close as possible to the real one. In the case of this suspension, the spring shock absorber is not connected to the lower arm as usual, but to the upper one.

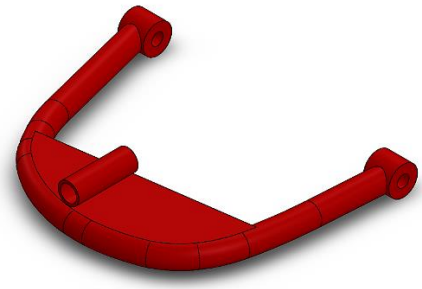

Figure 1. Geometry of the lower control arm.

2.2. Finite element analysis

The finite element method requires the appropriate definition of boundary conditions and generation of the mesh for the optimal convergence of the solution. The variables selected for the study were von Mises equivalent stress and total deformation (for the convergence studies).

2.2.1. Boundary conditions

The boundary conditions are the loads applied to the control arm and its supports. To obtain the reactions in the component that was analysed, a movement analysis was performed using SolidWorks Motion complement. In this process, the following parts of the system were modelled, see Figure 2:

- Upper control arm.
- Lower control arm.
- Spring shock absorber.
- Ball joints.

The steering knuckle, the part between the ball joints, was assumed as a rectangular plate. A quarter-vehicle model was taken into account for the study since it is a simple model but widely used in the literature [17]. The assembly shown in Figure 2 was used to calculate the reactions in the lower control arm. An upward vertical force of 1125 N was applied in the middle of the steering knuckle, this magnitude corresponds to a quarter of the weight of the vehicle (including passengers). For the model, the spring stiffness was 30 N/mm and the damping coefficient of the shock absorber was 0.22 Ns/mm. It was not necessary to make the geometric model of the spring since it was simulated by the software. The forces calculated were the reactions due to the contact with the ball joint.

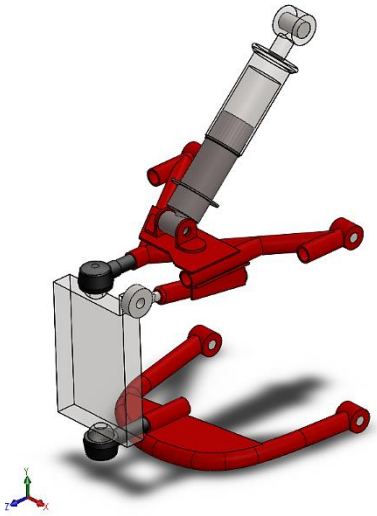

Figure 2. Suspension system modelled.

Through the movement analysis, curves that show the variation of the components of the force with respect to time were found. The results obtained for the calculation of the reaction forces in the lower control arm are shown in Figure 3. As expected, the forces in the *z*-component are the most significant, and the *x*-components are almost nil. Since the force was not constant, the stresses were calculated for two different times, thus, two analyses were carried out. The first one for the initial time and second one for the steady state. The forces used for both analyses are shown in Table 2. The supports considered for both analyses were cylindrical supports. These supports avoid rigid body motion for the static structural analysis. Figure 4 shows the positions were the supports and the force were applied for the first analysis. These positions were the same for the second analysis.

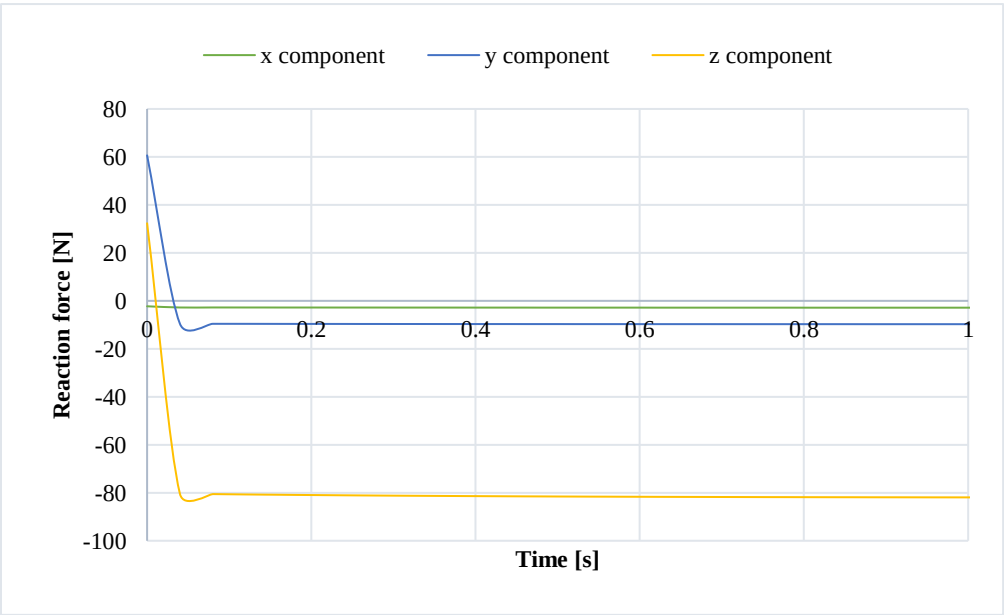

Figure 3. *x*-component, *y*-component and *z*-component of the force acting in the control arm.

Table 2. Forces applied for each analysis.

Component	First analysis	Second analysis
x-component	-2.3 N	-2.9 N
y-component	61 N	-10 N
z-component	32 N	-82 N

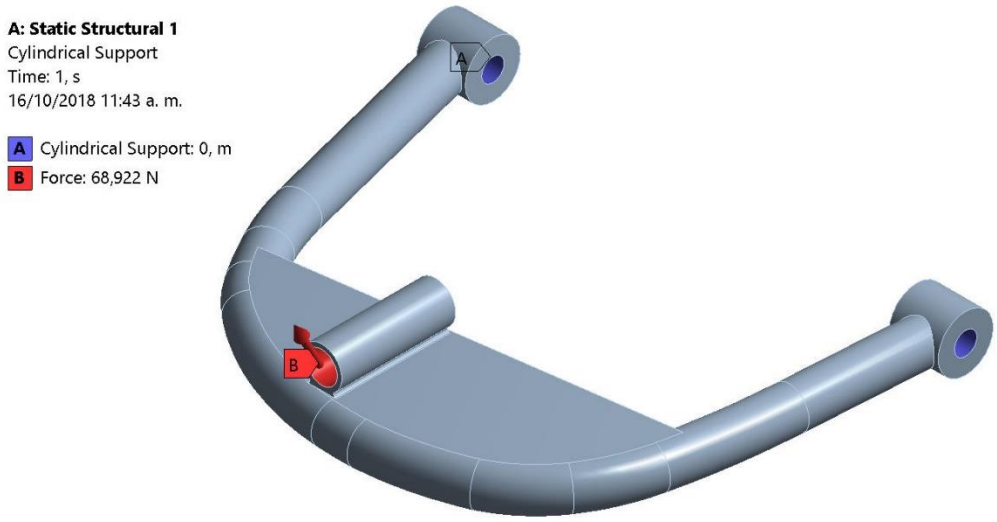

Figure 4. Boundary conditions for the first analysis.

2.2.2. Mesh

The initial mesh of the first analysis had 12811 nodes and 7047 elements, and the second had 12985 nodes and 7181 elements. The element types used were SOLID187 and SURF154. Within the configuration parameters of the mesh, the option Curvature was selected as Size Function. Although, after carrying out the convergence studies (Table 3 and Table 4), the fourth mesh was selected in both cases.

2.2.3. Mesh independence analysis

For finite element analysis (FEA), we should perform mesh independence verification by checking the convergence of the solution and establishing the appropriate element size. For this, we varied the size of the elements, or mesh density, and observed the change in the total deformation. The total deformation was chosen to perform the convergence because when performing it with the stress, singularities could affect convergence. The convergence curves are shown in Figure 5. It can be observed that, in both cases, the result of the maximum total deformation did not have a significant modification when changing from mesh 3 to 4. Thus, we considered the fourth mesh for the study. The data of the convergence study done for the first and second analysis are shown in Table 3 and Table 4, respectively.

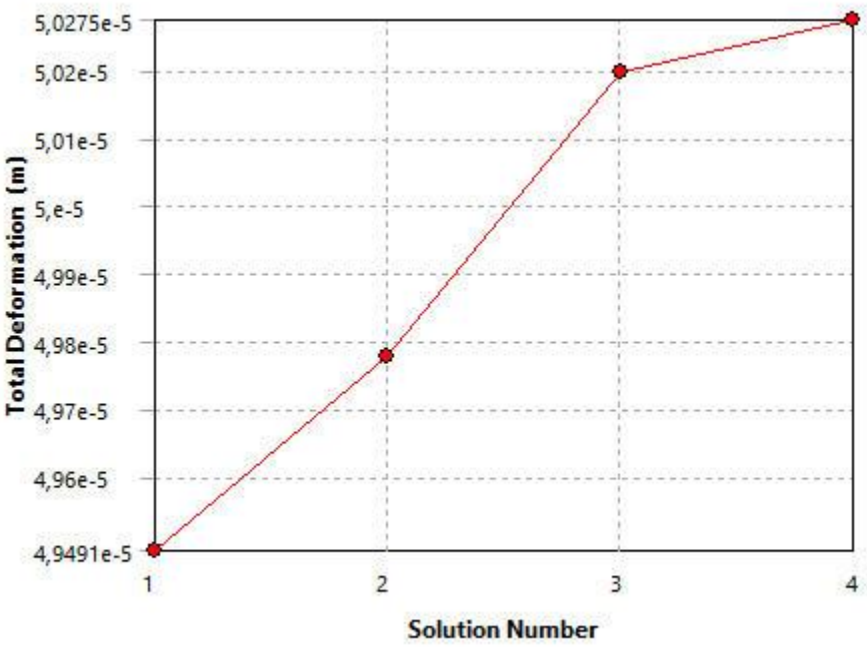

(a)

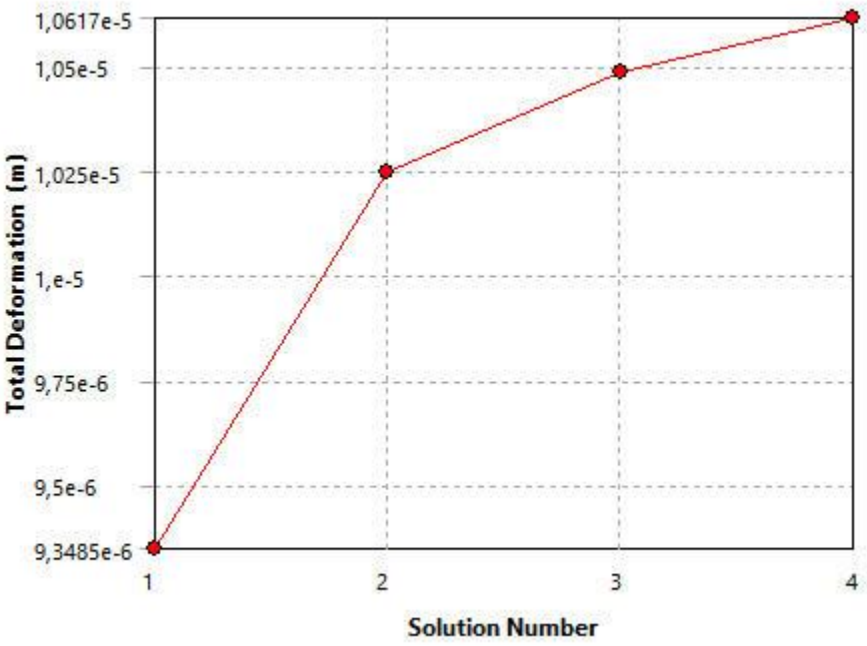

(b)

Figure 5. Convergence curves.

Table 3. First analysis convergence data.

Solution Number	Total Deformation (m)	Change (%)	Nodes	Elements
1	4.9491e-5	-	12811	7047
2	4.9778e-5	0.57795	29922	17402
3	5.0197e-5	0.83888	73205	45235
4	5.0275e-5	0.15369	200968	132658

Table 4. Second analysis convergence data.

Solution Number	Total Deformation (m)	Change (%)	Nodes	Elements
1	9.3485e-6	-	12985	7181
2	1.0248e-5	9.1838	34509	20293
3	1.0489e-5	2.321	69577	43433
4	1.0617e-5	1.2151	133224	86979

3. RESULTS

Figure 6 shows the results for the von Mises stress. The equivalent stress distribution for the first analysis had a maximum value of approximately 22 MPa (Figure 6a) and the second had a maximum of 20 MPa (Figure 6b). Both results are low taking into account the structural steel strength. In addition, the regions of the control arm where the highest stresses occur are small zones.

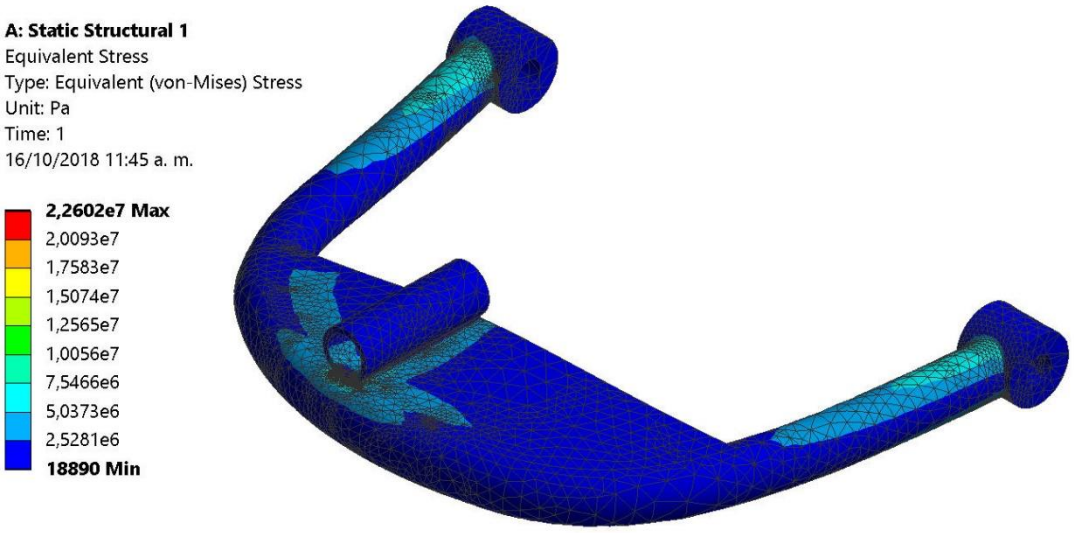

(a)

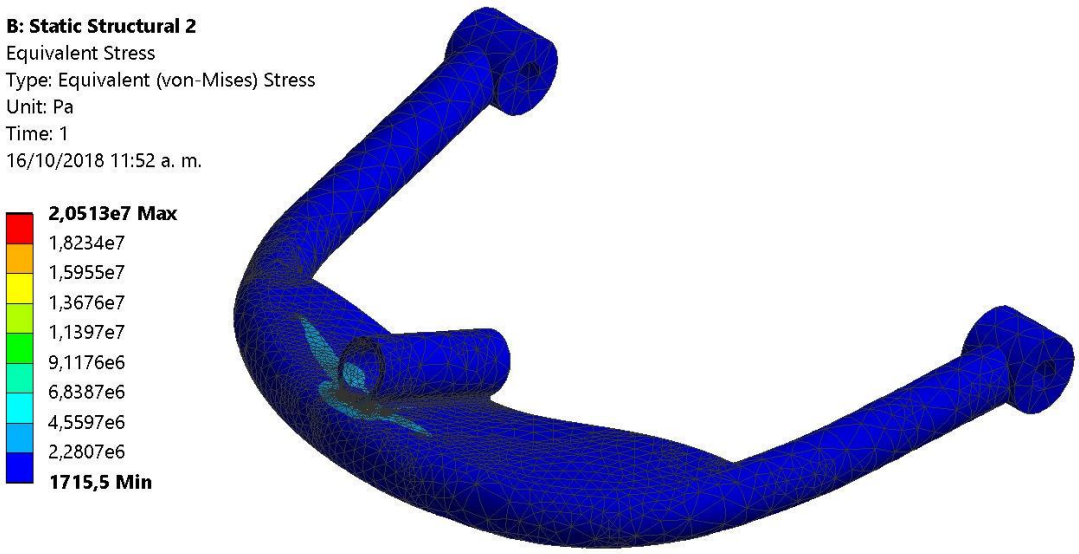

(b)

Figure 6. First (a) and second analysis (b) stress distribution.

Figure 7 shows the total deformation for both analyses. The maximum value for the first analysis was approximately 5e-5 m, and for the second 1e-5 m. Notice that the maximum values of the total deformation occur at different regions of the control arm, which is explained by the different direction of the force applied in each case.

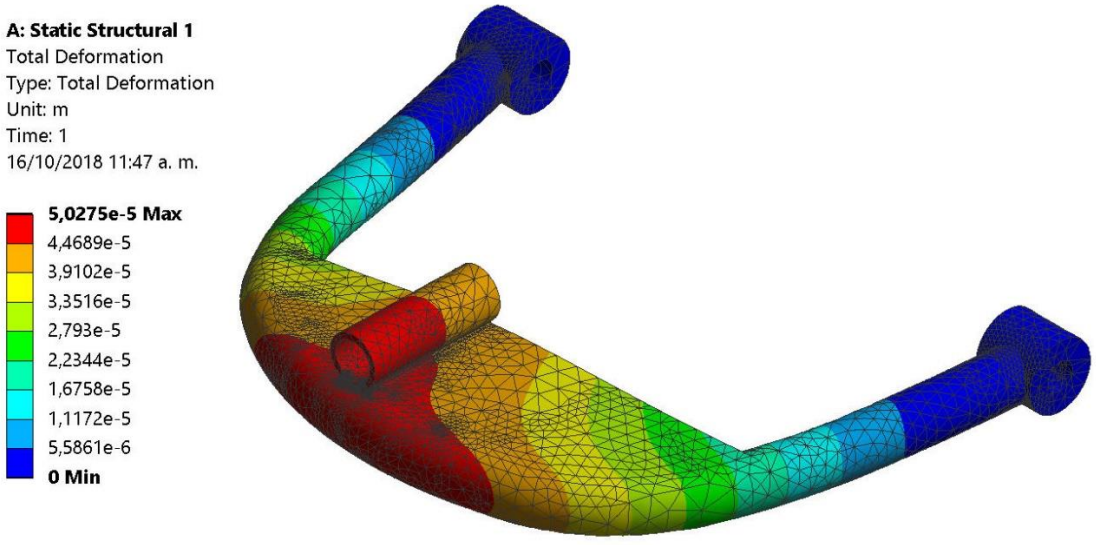

(a)

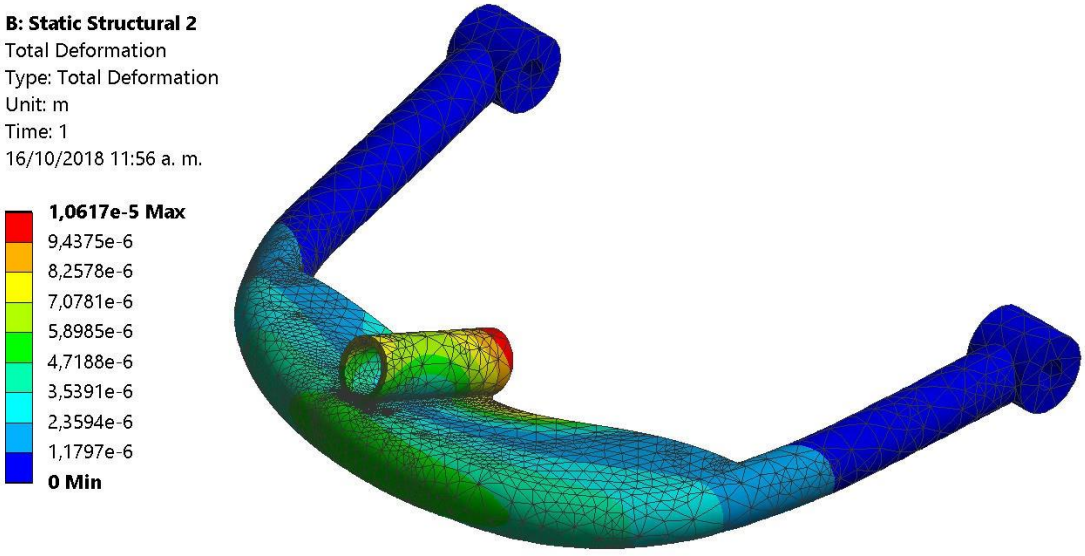

(b)

Figure 7. First (a) and second analysis (b) total deformation.

4. CONCLUSIONS

In this work, a FEA of a lower control arm was performed to obtain the equivalent stress distribution and the total deformation of the part under critical loading conditions. For this, the forces of interest acting in part were calculated. Then, the finite element model was developed, considering a convergence study of the mesh. The calculated loads of the control arm were low, within the range of 65 to 85 N and, therefore, there were also low stresses, close to 20 MPa. These results show that it would be suitable to study the possibility of optimising its shape to save material. Additionally, a possible change of material could also be evaluated since in this case the use of a material with the strength of the steel is not justified.
On the other hand, further studies could investigate more on the calculation of the loads to which the part is subjected since, in this study, only the weight of the vehicle was taken into account, but there are other conditions that may also affect the part.

5. REFERENCES

[1] E. Martínez, O. A. González-Estrada, and A. Martínez, "Evaluación de las propiedades tribológicas de materiales compuestos de matriz metálica (MMCs) procesados por técnicas de fabricación aditiva con haz láser (SLM)," *Rev. UIS Ing.*, vol. 16, no. 1, pp. 101–114, 2017, doi:10.18273/revuin.v16n1-2017010.

[2] O. A. González-Estrada, G. Díaz, and J. E. Quiroga Mendez, "Mechanical Response and Damage of Woven Composite Materials Reinforced with Fique," *Key Eng. Mater.*, vol. 774, pp. 143–148, 2018, doi:10.4028/www.scientific.net/KEM.774.143.

[3] J. S. León B, O. A. González-Estrada, and A. Pertuz, "Damage in Fibreglass Composite Laminates Used for Pipes," *Key Eng. Mater.*, vol. 774, pp. 155–160, 2018, doi:10.4028/www.scientific.net/KEM.774.155.

[4] O. A. González-Estrada, A. Pertuz, and J. E. Quiroga Mendez, “Evaluation of Tensile Properties and Damage of Continuous Fibre Reinforced 3D-Printed Parts,” *Key Eng. Mater.*, vol. 774, pp. 161–166, 2018, doi:10.4028/www.scientific.net/KEM.774.161.

[5] K. Molina, D. Ortega, M. Martínez, W. Pinto Hernández, and O. A. González-Estrada, “Modelado de la interacción fluido estructura (FSI) para el diseño de una turbina eólica HAWT,” *Rev. UIS Ing.*, vol. 17, no. 2, pp. 269–282, 2018, doi:10.18273/revuin.v17n2-2018023.

[6] Á. O. Díaz-Rey, J. E. González-Gil, O. A. González-Estrada, Á. Díaz Rey, J. González Gil, and O. A. González-Estrada, “Análisis de un generador de HHO de celda seca para su aplicación en motores de combustión interna,” *Rev. UIS Ing.*, vol. 17, no. 1, pp. 143–154, 2018, doi:10.18273/revuin.v17n1-2018013.

[7] Y. J. Rueda Ordóñez, K. K. Tannous, Y. Rueda-Ordóñez, and K. K. Tannous, “Análisis cinético de la descomposición térmica de Biomasa aplicando un esquema de reacciones paralelas independientes,” *Rev. UIS Ing.*, vol. 16, no. 2, pp. 119–128, 2017, doi:https://doi.org/10.18273/revuin.v16n2-2017011.

[8] G. González, N. Prieto, and I. Mercado, “Large Eddy Simulation (LES) Aplicado a un lecho fluidizado gas – sólido . Parte I : Reactor a escala de laboratorio,” *Rev. UIS Ing.*, vol. 17, no. 1, pp. 93–104, 2018, doi:https://doi.org/10.18273/revuin.v17n1-2018009.

[9] A. Ramirez-Matheus, M. Díaz-Rodríguez, and O. A. González-Estrada, “Estrategia de optimización para la síntesis dimensional de un robot paralelo 5R para una aplicación de mesa de corte,” *Rev. UIS Ing.*, vol. 16, no. 2, pp. 197–206, 2017, doi:10.18273/revuin.v16n2-2017018.

[10] A. Ayestarán, C. Graciano, and O. A. González-Estrada, “Resistencia de vigas esbeltas de acero inoxidable bajo cargas concentradas mediante análisis por elementos finitos,” *Rev. UIS Ing.*, vol. 16, no. 2, pp. 61–70, Sep. 2017, doi:10.18273/revuin.v16n2-2017006.

[11] Y. Jin, O. A. González-Estrada, O. Pierard, and S. P. A. Bordas, “Error-controlled adaptive extended finite element method for 3D linear elastic crack propagation,” *Comput. Methods Appl. Mech. Eng.*, vol. 318, pp. 319–348, 2017, doi:10.1016/j.cma.2016.12.016.

[12] S. A. Ardila Parra, O. A. González-Estrada, and J. E. Quiroga Mendez, “Damage Assessment of Spinal Bones due to Prostate Cancer,” *Key Eng. Mater.*, vol. 774, pp. 149–154, 2018, doi:10.4028/www.scientific.net/KEM.774.149.

[13] O. A. González-Estrada, S. Natarajan, and C. Graciano, “Reconstrucción de tensiones para el método de elementos finitos con mallas poligonales,” *Rev. UIS Ing.*, vol. 16, no. 1, pp. 23–34, 2017, doi:10.18273/revuin.v16n1-2017003.

[14] A. P. N. Vivekanandan, A. Gunaki, C. Acharya, S. Gilbert, and R. Bodake, “Design , Analysis and Simulation of Double Wishbone Suspension System,” *Int. J. Mech. Eng.*, vol. 2, no. 6, pp. 1–7, 2014.

[15] R. N. Jazar, *Vehicle Dynamics*. New York: Springer, 2014.

[16] E. Madenci and I. Guven, *The Finite Element Method and Applications in Engineering Using ANSYS*. New York: Springer, 2015.

[17] M. Bouazara, “Improvement in the Design of Automobile Upper Suspension Control Arms Using Aluminum Alloys,” *Damage Fract. Mech.*, pp. 101–112, 2009, doi:10.1007/978-90-481-2669-9_11.